Geomicrobiology Journal
Publication details, including instructions for authors and subscription information:
http://www.tandfonline.com/loi/ugmb20

Speciation-Dependent Kinetics of Uranium(VI) Bioreduction

Kai-Uwe Ulrich [a], Harish Veeramani [b], Rizlan Bernier-Latmani [b] & Daniel E. Giammar [a]
[a] Department of Energy, Environmental and Chemical Engineering, Washington University, St. Louis, Missouri, USA
[b] Ecole Polytechnique Fédérale de Lausanne, Lausanne, Switzerland

Available online: 26 Jul 2011

To cite this article: Kai-Uwe Ulrich, Harish Veeramani, Rizlan Bernier-Latmani & Daniel E. Giammar (2011): Speciation-Dependent Kinetics of Uranium(VI) Bioreduction, Geomicrobiology Journal, 28:5-6, 396-409

To link to this article: http://dx.doi.org/10.1080/01490451.2010.507640

Geomicrobiology Journal, 28:396–409, 2011

ISSN: 0149-0451 print / 1521-0529 online
DOI: 10.1080/01490451.2010.507640

Taylor & Francis
Taylor & Francis Group

Speciation-Dependent Kinetics of Uranium(VI) Bioreduction

Kai-Uwe Ulrich,[1] Harish Veeramani,[2] Rizlan Bernier-Latmani,[2] and Daniel E. Giammar[1]

[1]*Department of Energy, Environmental and Chemical Engineering, Washington University, St. Louis, Missouri, USA*
[2]*Ecole Polytechnique Fédérale de Lausanne, Lausanne, Switzerland*

The kinetics of uranium(VI) reduction by *Shewanella oneidensis* strain MR-1 was studied for varied pH and concentrations of dissolved inorganic carbon (DIC) and calcium. These are key variables affecting U(VI) speciation in aqueous systems. For all conditions studied, a nearly log-linear decrease of [U(VI)] suggested pseudo–first-order kinetics with respect to U(VI). The reduction rate constants (k) decreased with increasing DIC and calcium concentration, and were sensitive to pH. A positive correlation was found between k and the logarithm of the total concentration of U(VI)-hydroxyl and U(VI)-organic complexes. Linear correlations of the rate constant with the redox potential (E_H) of U(VI) reduction and the associated Gibbs free energy of reaction (ΔG_r) were found for both Ca-free and Ca-containing systems. Both E_H and ΔG_r are strong functions of aqueous U(VI) speciation. Because the range in ΔG_r among the experimental conditions was small, the differences in k are more likely to be due to differences in E_H or to differences in individual rate constants of U(VI) species. Calculation of conditional reduction rate constants for the major groups of U(VI) complexes revealed highest constants for the combined groups of U(VI)-hydroxyl and U(VI)-organic species, lower rate constants for the U(VI)-carbonate group, and much lower constants for the Ca-U(VI)-carbonate group. Mechanistic explanations for these findings are discussed.

Keywords uranium(VI), aqueous speciation, bioreduction, reduction kinetics, *Shewanella oneidensis* MR-1

INTRODUCTION

Past activities of mining and processing uranium ores, manufacturing and testing nuclear weapons, and nuclear accidents, as well as other activities such as the use of phosphate fertilizers, have led to uranium-contaminated soil and groundwater. Uranium in its oxidized hexavalent form, U(VI), can be highly soluble in water over a wide pH range and thus largely mobile in the subsurface. The solubility of tetravalent uranium species is lower by several orders of magnitude and usually controlled by uraninite (UO_2). In anoxic aqueous systems, reduction of U(VI) to UO_2 can occur either chemically, e.g., by hydrogen sulfide (Hua et al. 2006), by surface catalyzed reactions involving coadsorption of Fe(II) and U(VI) on iron(III) oxides (Behrends and Van Cappellen 2005; Fredrickson et al. 2000; Jeon et al. 2005), or microbially, i.e., catalyzed by enzymes.

Several groups of metal- and sulfate-reducing bacteria of diverse phylogenetic origin, e.g., Gammaproteobacteria, Deltaproteobacteria, Actinobacteria, and Firmicutes (Lloyd et al. 2002; Lovley et al. 1991; Suzuki and Suko 2006) are known to mediate U(VI) reduction. Based on these discoveries, the concept of *in situ* bioremediation was developed: by stimulation of indigenous U(VI)-reducing bacteria in the subsurface through the amendment of organic electron donors such as acetate, ethanol, or lactate, U(VI) will be transformed into an immobile *in situ* solid waste form (Abdelouas et al. 1999). This concept was initially tested in the laboratory by using pure cultures or complex media from field sites, and it has been tested in the field (Anderson et al. 2003; Gu et al. 2005; N'Guessan et al. 2008; Senko et al. 2002; Wu et al. 2006).

The rate of microbial U(VI) reduction will depend on the environment in which the bacteria live, in particular on aqueous chemistry and temperature. Other factors may include the type and electron transfer reactions of specific enzymes that catalyze U(VI) reduction. Hence, dependencies are expected to vary across microbial species and strains, and optimum conditions are likely to depend on the specific site conditions. Dissolved U(VI) is considerably more bioavailable for reduction than adsorbed and precipitated or solid-phase U(VI) (Liu et al. 2006; Ortiz-Bernad et al. 2004), which is analogous to the trend of soluble Fe(III) being more bioavailable and thus rapidly reduced by microorganisms than solid-phase Fe(III) oxides (Liu et al. 2002).

For soluble U(VI) species, little is known about the effects of aqueous chemistry and uranium speciation on microbially catalyzed uranium reduction. Previous investigations showed a tremendous inhibition of U(VI) bioreduction with increasing Ca^{2+} concentration, consistent with the hypothesis that

Received 15 January 2010; accepted 6 July 2010.
Address correspondence to Dr. Kai-Uwe Ulrich, BGD Soil and Groundwater Laboratory GmbH, Tiergartenstrasse 48, 01219 Dresden, Germany. E-mail: kulrich@bgd-gmbh.de

Ca-U(VI)-carbonate ternary complexes are less energetically favorable for enzymatic U(VI) reduction than Ca-free U(VI)-complexes (Brooks et al. 2003; Luo et al. 2007; Neiss et al. 2007; Stewart et al. 2007). This effect was exemplified for one facultative (*Shewanella putrefaciens* strain CN32) and two obligate anaerobes (*Desulfovibrio desulfuricans* and *Geobacter sulfurreducens*) (Brooks et al. 2003; Neiss et al. 2007; Stewart et al. 2007).

While the above investigations were carried out at neutral pH and fixed carbonate concentrations, two additional studies demonstrated the inhibition of U(VI) bioreduction by dissolved inorganic carbon (DIC). Investigating the kinetics of abiotic U(VI) reduction by hydrogen sulfide in anoxic aqueous systems, Hua et al. (2006) reported that the reduction was almost completely inhibited at the following conditions: [DIC] $\geq$ 15 mM at pH 6.89, [DIC] $\geq$ 4 mM at pH 8.01, and [DIC] $\geq$ 2 mM at pH 9.06. These combinations of DIC concentrations and pH suggest an anti-correlation between the concentration of U(VI)-carbonate complexes and reduction rate.

In fact, the authors found a strong positive correlation between the initial rate of U(VI) reduction and the total concentrations of U(VI)-hydroxyl species. This observation led to the conclusion that sulfide reduced the U(VI)-hydroxyl species, but not the dominant U(VI)-carbonate complexes that are present in many carbonate-containing systems. In the second study (Behrends and Van Cappellen 2005), addition of 45 mM HCO_3^- considerably impeded the reduction of U(VI) in abiotic systems containing soluble Fe(II) and hematite. A similar effect was observed in systems containing soluble Fe(II), *Shewanella putrefaciens* cells, and lactate as an electron donor. Although details of this study cannot be considered here, the overall results showed that the inhibitory effect was neither restricted to direct enzymatic nor to surface-catalyzed U(VI) reduction. Rather, it appeared to be consistent with the formation of sorption-resistant aqueous U(VI)-carbonate complexes.

In summary, these studies demonstrate that speciation of U(VI) is key to its bioavailability and susceptibility to bioreduction. The objective of the present study is to expand the knowledge of the effects of aqueous chemistry and speciation on the bioavailability and bioreduction of U(VI) by using a more systematic approach and a microorganism (*Shewanella oneidensis* strain MR-1) that has not yet been studied in this respect. Our investigation considers the effects of carbonate and calcium concentrations and pH which are major chemical parameters affecting U(VI) speciation. The ultimate goal is to identify the key chemical factors that affect U(VI) bioreduction and to develop a simple rate equation for purposes of field applications.

MATERIALS AND METHODS

Experimental Setup and Conditions

Biological uranium reduction experiments were conducted in an anaerobic chamber (Coy Laboratory Products) maintaining a controlled gas atmosphere (3% hydrogen, 97% nitrogen) and equipped with a palladium catalyst to scrub remaining traces of oxygen. Serum bottles with 200 or 500 mL capacity were used as reactors and amended with the appropriate volumes (headspace/liquid ratio = 1) and final concentrations (accounting for all dilutions from sterile stock solutions) of 1 to 50 mM sodium bicarbonate, 20 mM lactic acid, 0 to 5 mM calcium chloride, and 0 or 20 mM PIPES (piperazine-N,N′-bis(2-ethanesulfonic acid)) according to Table 1. For the set of experiments with varied calcium concentrations, pH 6.8 or 6.3 was set by continuously purging a gas mixture of 25 or 45 vol% CO_2 (balance N_2) through the batch solutions for several hours, and no pH buffer was used. When the pH appeared stable, the gas flow was maintained for one more hour to test the stability of the calculated equilibrium pH (6.82 or 6.29 for the given conditions). The reactors were sealed quickly and autoclaved.

The microbial cultures were prepared under ambient conditions as follows. A frozen stock culture (-80°C) of *Shewanella oneidensis* MR-1 was streaked onto a petri-dish containing sterile Luria-Bertani (LB) agar and incubated for 24 h at 30°C. A single colony was picked using a sterile plastic loop and inoculated into a 15 mL test-tube containing 10 mL sterile LB broth and incubated for 12 hours on an incubated shaker (New Brunswick Scientific – Excella Benchtop Incubator Shakers) at 30°C (140 rpm). The 12-hour culture was then re-inoculated into a 2 liter baffled Fernbach flask containing 1 L sterile LB broth and incubated under the same conditions as above.

After approximately 12 hours, the optical density of the suspension was measured at a wavelength of 600 nm (OD_{600}). An OD_{600} value of $\sim$3 indicated that the desired bacterial biomass for the batch experiments was reached at the late log-phase. Both the test-tube and the baffled Fernbach flask were equipped with standard lids that minimized gas exchange with the atmosphere while ensuring sterility. Due to rapid O_2 consumption by the bacteria, the culture was oxygen limited. Diffusion of O_2 into the medium likely was the rate-limiting step in the growth. However, the conditions never became anaerobic based on the fact that the cells never turned bright red. Under anaerobic conditions, strain MR-1 cells express numerous cytochromes and turn bright red.

The cell suspension was centrifuged at 10,000 *g* for 20 min and the pellet was washed twice in the above-mentioned reduction matrix composed of sodium bicarbonate, PIPES, lactate and devoid of calcium to prime the bacterial cells for the experimental conditions. The washed pellet was re-suspended in a small volume of reduction matrix and thoroughly mixed. A small calculated volume of the cell suspension was transferred to the serum bottles using a sterile syringe to get a similar cell density in all the reactors. The cell density was verified as described above.

An OD_{600} value of 2.0 ± 0.05 corresponded to a mean cell density of $21 \pm 2 \cdot 10^7$ cells/mL and a protein concentration of 120.8 ± 3.3 mg/L as determined by the Bradford assay. The cell suspensions were allowed to incubate in the reduction matrix

TABLE 1
Experimental conditions for which rate constants were determined for U(VI) reduction by *Shewanella oneidensis* MR-1. Gibbs free energy of reaction (ΔG_r) as well as redox potential (E_H) are calculated for each condition

Condition														
Fixed pH	6.3	6.3	6.3	6.3	6.3	6.3	6.3	6.3	6.3*	6.3	6.8*	6.8*	6.8*	8.0*
PIPES buffer (mM)	20	20	20	20	20	20	0	0	0	0	0	0	0	20
[$CaCl_2$] (mM)	0	0	0	0	0	0	0	0.5	1.0	5.0	0	0.5	5.0	0
[$NaHCO_3$] (mM)	1.0	5.0	10	20	30	50	15	15	15	15	30	30	30	30
[$CO_{2(g)}$]$_0$ (bar)	0#	0#	0#	0#	0#	0#	0.456	0.456	0.456	0.456	0.253	0.253	0.253	0#
Calculated DIC (mM)	1.0	5.0	10	20	30	50	35	35	35	36	42	42	43	31
[U(VI)hyd]$_0$ (M)	$2.86 \cdot 10^{-5}$	$1.67 \cdot 10^{-6}$	$6.06 \cdot 10^{-7}$	$1.47 \cdot 10^{-7}$	$4.84 \cdot 10^{-8}$	$9.40 \cdot 10^{-9}$	$4.12 \cdot 10^{-8}$	$2.64 \cdot 10^{-8}$	$1.50 \cdot 10^{-8}$	$6.10 \cdot 10^{-10}$	$1.09 \cdot 10^{-9}$	$6.62 \cdot 10^{-10}$	$1.82 \cdot 10^{-11}$	$2.55 \cdot 10^{-11}$
[U(VI)org]$_0$ (M)	$3.53 \cdot 10^{-6}$	$1.19 \cdot 10^{-6}$	$6.72 \cdot 10^{-7}$	$2.12 \cdot 10^{-7}$	$7.04 \cdot 10^{-8}$	$1.34 \cdot 10^{-8}$	$6.21 \cdot 10^{-8}$	$3.99 \cdot 10^{-8}$	$2.27 \cdot 10^{-8}$	$9.11 \cdot 10^{-10}$	$4.00 \cdot 10^{-10}$	$2.43 \cdot 10^{-10}$	$6.63 \cdot 10^{-12}$	$4.45 \cdot 10^{-14}$
[U(VI)carb]$_0$ (M)	$4.69 \cdot 10^{-4}$	$5.87 \cdot 10^{-4}$	$7.05 \cdot 10^{-4}$	$8.53 \cdot 10^{-4}$	$9.14 \cdot 10^{-4}$	$9.70 \cdot 10^{-4}$	$9.32 \cdot 10^{-4}$	$5.92 \cdot 10^{-4}$	$3.37 \cdot 10^{-4}$	$1.47 \cdot 10^{-5}$	$9.99 \cdot 10^{-4}$	$6.12 \cdot 10^{-4}$	$1.85 \cdot 10^{-5}$	$4.00 \cdot 10^{-4}$
[CaU(VI)carb]$_0$ (M)	0	0	0	0	0	0	0	$3.88 \cdot 10^{-4}$	$6.60 \cdot 10^{-4}$	$9.85 \cdot 10^{-4}$	0	$3.87 \cdot 10^{-4}$	$9.82 \cdot 10^{-4}$	0
Rate constant (h^{-1})	1.07	0.79	0.67	0.58	0.62	0.1	0.28	0.23	0.21	0.09	0.17	0.15	−0.01$	0.06
ΔG_r (kJ/mol)	−603	−595	−592	−587	−584	−578	−583	−582	−580	−572	−572	−571	−562	−559
E_H (V)	0.026	0.012	0.006	−0.008	−0.021	−0.041	−0.024	−0.030	−0.037	−0.078	−0.087	−0.094	−0.140	−0.203

*No replicate carried out. #No external $CO_{2(g)}$ flushed through the reactor. $No U(VI) reduction observed within first 6 h; [U(VI)] increase within experimental error. Initially constant parameters include lactic acid (20 mM) and uranyl acetate (1.0–1.2 mM) except for the pH 8.0 condition, which used 0.4 mM uranyl acetate and 50% of the standard biomass. Alkalinity was fixed by the concentration of $NaHCO_3$. For some systems, a controlled partial pressure of $CO_{2(g)}$ was applied to the vials' headspace to adjust the pH. For each system, the total concentrations of DIC and U(VI) species were calculated for the groups of U(VI)-hydroxyl, U(VI)-organic, U(VI)-carbonate, and Ca-U(VI)-carbonate complexes (Table 2). Replicates were performed except where noted.

for 30 minutes prior to addition of U(VI) to allow the cells to adapt to the strictly anaerobic conditions and express c-type cytochromes. The reactors were finally amended with ~1 mM U(VI) from a sterile stock of 10 mM uranyl acetate solution. The bottles were swirled to ensure uniform mixing of the uranium and the bacterial biomass. The experiments were performed in replicates except where noted (Table 1).

A control experiment was performed in parallel in which the bacteria were killed by treating them with a 4% formaldehyde solution for 60 min. Full recovery of dissolved U(VI) over the course of this control experiment (cf. Figure 4c) ruled out both sorption of U(VI) to the biomass or container walls and abiotic reduction of U(VI) as possible pathways for loss of dissolved U(VI). These experiments demonstrated the need for live bacteria to have U(VI) reduced under the given conditions.

Samples were periodically withdrawn using sterile syringes and needles, and filtered using a 0.2 μm filter (polyethersulfone). Disappearance of U(VI) from solution was monitored by determining the aqueous U(VI) concentration with a kinetic phosphorescence analyzer (KPA, Chemchek Instruments). The pH was monitored over the course of the experiment; no significant change was observed within the methodological uncertainty (±0.02 pH units). The experimental conditions of all U(VI) reduction experiments are summarized in Table 1.

Reduction Rate Calculation

Reduction was examined as a first-order kinetic process with respect to [U(VI)] (Eq. (1)). The reduction rate may also depend on the cell density. However, due to non-growth conditions, cell density can be assumed constant over the time course of the experiments. Thus, the overall rate may be considered to be pseudo-first order.

$$\left(\frac{d[U(VI)]}{dt}\right) = -k[U(VI)] \qquad [1]$$

Although the overall rates of microbial metal reduction may strictly follow Monod or Michaelis-Menten kinetics, at non-growth conditions a first-order rate model approximation of Monod kinetics has been demonstrated to provide equally good fits to experimental data as Monod kinetics (Liu et al. 2002). Other studies of microbial U(VI) reduction rates have also found good fits of first-order rate models to experimental data (Stewart et al. 2007). Rearrangement of the integrated form of equation 1 allows the first-order rate constant k to be determined from a linear regression of the natural logarithm of $[U(VI)]/[U(VI)]_0$, the ratio of U(VI) remaining at time t and the total uranium (at time zero) versus time (Eq. (2)),

$$\ln\left(\frac{[U(VI)]}{[U(VI)]_0}\right) = -kt \qquad [2]$$

This approach is first presented only in terms of the total concentration of dissolved uranium. However, we may hypothesize individual reduction rates for each U(VI) species. As a first estimate, we assume different conditional rates (in h^{-1}) for characteristic groups of U(VI) species, i.e., U(VI)-hydroxyl, U(VI)-organic, U(VI)-carbonate, and Ca-U(VI)-carbonate complexes. Subsequently, the names of these groups are abbreviated by U(VI)hyd, U(VI)org, U(VI)carb, and CaU(VI)carb. The overall U(VI) reduction rate constant k (h^{-1}) can then be obtained from the combination of group-specific conditional rates k_1 to k_4 according to Equation (3),

$$k = \frac{k_1 \sum \{U(VI)hyd\} + k_2 \sum \{U(VI)org\} + k_3 \sum \{U(VI)carb\} + k_4 \sum \{CaU(VI)carb\}}{\{U(VI)\}} \qquad [3]$$

Thermodynamic Calculations

Reduction of U(VI) by *Shewanella oneidensis* is coupled to the oxidation of the electron donor lactate, which was supplied in excess. Under anaerobic near-neutral conditions, lactate will be oxidized to acetate and HCO_3^- rather than completely mineralized to CO_2 and H_2O. The generic form of the overall redox reaction is given by Equation (4).

$$2\ UO_2^{2+} + CH_3CH(OH)COO^- + 2\ H_2O \leftrightarrow CH_3COO^- + HCO_3^- + 2\ UO_{2(s)} + 5\ H^+ \qquad [4]$$

The feasibility of a reaction will be dependent on the Gibbs free energy of reaction, which is controlled by the Gibbs energy of formation and the activity of the individual species reacting under given chemical conditions,

$$\Delta G_r = \Delta G_r^o + RT \ln Q \qquad [5]$$

where ΔG_r is the Gibbs free energy of the reaction at the actual conditions, ΔG_r^o is the standard Gibbs free energy of the reaction calculated from the standard Gibbs free energies of formation data taken from literature (Guillaumont et al. 2003; Sawyer et al. 2003) and Q is the reaction quotient according to Equation (6).

$$Q = \frac{\{CH_3COO^-\}\{HCO_3^-\}\{H^+\}^5}{\left\{UO_2^{2+}\right\}\{CH_3CH(OH)COO^-\}} \qquad [6]$$

The ion activities in Eq. (6) were calculated using the Environmental Research software MINEQL$^+$ (Schecher and McAvoy 1998) as discussed in the next section.

In the case of redox reactions, the Gibbs free energy of an overall reaction is proportional to the difference between the redox potentials of the electron donor and electron acceptor half-cell reactions. For the U(VI) reduction half-reaction shown in Equation (7), the effective redox potentials E_H for different conditions were calculated by using the Nernst Equation (Eq. (8)) where n is the number of electrons transferred and E_H^o

is the standard-state half-cell potential.

$$UO_2^{2+} + 2e^- \leftrightarrow UO_{2(s)} \quad [7]$$

$$E_H = E_H^\circ - \frac{0.059}{n} \log\left(\frac{1}{\{UO_2^{2+}\}}\right) \quad [8]$$

The value of 0.222 V for E_H^o was determined from values reported in the NEA thermodynamic database (Guillaumont et al. 2003) using $UO_{2(am)}$ as the U(IV) product of reduction, which is consistent with previous measurements of biogenic UO_2 solubility (Ulrich et al. 2009).

Speciation Calculations

Speciation of U(VI) was calculated using the Environmental Research software MINEQL$^+$ (Schecher and McAvoy 1998) and the most recent NEA thermodynamic database for uranium hydrolysis and carbonate complexes (Guillaumont et al. 2003). For calcium-uranyl-carbonate species and uranyl lactate (UO_2Lac^+), equilibrium constants extrapolated to zero ionic strength were taken from Dong and Brooks (2006) and Moore et al. (1999) (using data based on the Pitzer ionic interaction model). The dissociation constant of lactic acid was taken from Partanen et al. (2003). The DIC concentration was calculated from the fixed alkalinity and the estimated equilibrium pH.

The formation of solids was not considered in the calculations, but the saturation indices of all potentially forming minerals were checked, and most of the solutions were undersaturated with respect to all possible U-containing solids. The ionic strength (*IS*) was fixed to the value calculated from concentrations of ions in the system (Table 1) and then used to determine the activity coefficients according to the Davies Equation (this step is implemented in MINEQL). From the output summary of all species for a single MINEQL run, total concentrations of U(VI) species were calculated for the groups of U(VI)hyd, U(VI)org, U(VI)carb, and CaU(VI)carb complexes and related to the experimental U(VI) reduction rates. Assuming fundamentally different kinetics for the different groups of U(VI) species, the group-specific reduction rate constants were calculated from Equation (3) using a weighted minimization of the residual sum of squares approach implemented with the Excel Solver tool.

RESULTS

U(VI) Speciation Calculations

Within the pH range from 6 to 8 at which the U(VI) reduction experiments were conducted with 1 mM TOTU, equilibrium calculations showed that U(VI) speciation is strongly affected by the DIC and calcium concentrations. In the absence of calcium, at a low DIC concentration of 1 mM and pH 6.3, U(VI) speciation is dominated by the complex $(UO_2)_2CO_3(OH)_3^-$ (88%), followed by the complex $(UO_2)_3(OH)_5^+$ (6.3%) (Figure 1a). At a higher DIC concentration of 35 mM, the uranyl carbonate species $UO_2(CO_3)_2^{2-}$ and $UO_2(CO_3)_3^{4-}$ are predominant above pH 6 (Figure 1b). However, in the presence of 5 mM calcium, the predominant species become $Ca_2UO_2(CO_3)_{3(aq)}$ and $CaUO_2(CO_3)_3^{2-}$ (Figure 1c).

These two Ca-containing uranyl complexes exhibit very similar proportions at pH 6.3 and 6.8: 68% vs. 67% of $Ca_2UO_2(CO_3)_{3(aq)}$ and 30.6 vs. 31.9% of $CaUO_2(CO_3)_3^{2-}$. In contrast, U(VI) speciation is more variable in the absence of calcium. Although at pH 6.8 $UO_2(CO_3)_2^{2-}$ and $UO_2(CO_3)_3^{4-}$ comprise 99.9% of the total dissolved uranium, two polymeric uranyl carbonate species [$(UO_2)_3(CO_3)_6^{6-}$ and $(UO_2)_2CO_3(OH)_3^-$] also contribute to U(VI) speciation at pH 6.3, together accounting for 10.6% of dissolved U(VI) (Figure 1b).

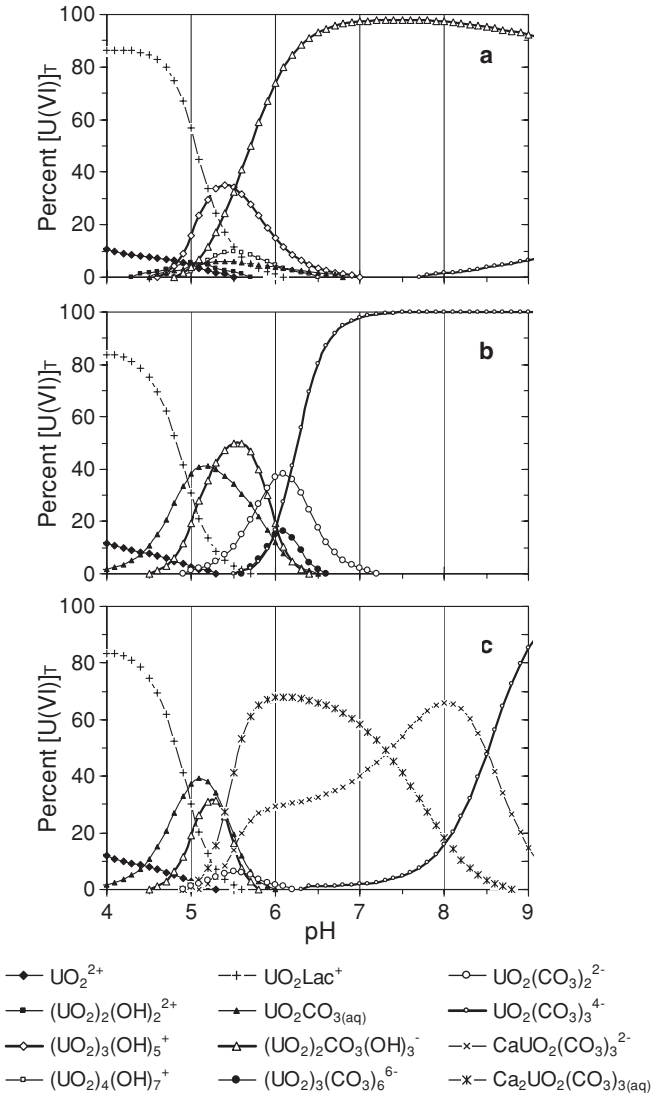

FIG. 1. U(VI) aqueous speciation as a function of pH for closed systems containing 1 mM uranyl acetate, 20 mM lactic acid, and (a) 1 mM DIC, no calcium; (b) 35 mM DIC, no calcium; (c) 35 mM DIC, 5 mM $CaCl_2$. Only species with ≥5% significance are shown; solids are not considered in speciation calculations.

TABLE 2
Stoichiometric formation constants (K_f at 298.15 K, extrapolated to zero ionic strength) of relevant reactions considered in addition to the reactions included in the NEA database (Guillaumont et al. 2003)

Reaction	Log K_f	Reference
$Lac^- + H^+ = HLac$	3.86	Partanen et al. (2003)
$Ace^- + H^+ = HAce$	4.757	Schecher and McAvoy (1998)
$Ace^- + Na^+ = NaAce_{(aq)}$	−0.18	Schecher and McAvoy (1998)
$Ace^- + Ca^{2+} = Ca(Ace)^+$	1.18	Schecher and McAvoy (1998)
$Lac^- + UO_2^{2+} = UO_2(Lac)^+$	3.09*	Moore et al. (1999)
$Ace^- + UO_2^{2+} = UO_2(Ace)^+$	3.03*	Moskvin et al. (1969), Moore et al. (1999)
$2\ Ace^- + UO_2^{2+} = UO_2(Ace)_2$	5.57	Moskvin et al. (1969)
$3\ Ace^- + UO_2^{2+} = UO_2(Ace)_3^-$	7.25	Moskvin et al. (1969)
$Ca^{2+} + 3\ CO_3^{2-} + UO_2^{2+} = CaUO_2(CO_3)_3^{2-}$	27.18	Dong and Brooks (2006)
$2\ Ca^{2+} + 3\ CO_3^{2-} + UO_2^{2+} = Ca_2UO_2(CO_3)_{3(aq)}$	30.70	Dong and Brooks (2006)

*Pitzer ionic interaction parameters used by Moore et al. (1999).

If lactate is the only electron donor and U(VI) the only acceptor in the system, changes in the lactate concentration will have a minimal effect on U(VI) speciation within the investigated pH range. Based on the thermodynamic constants obtained from the literature (Table 2), the uranyl lactate complex UO_2Lac^+ is expected to negligibly contribute to the overall speciation of U(VI) above pH 6 both at the onset and midpoint of the reduction reaction (with 0.5 mM U(VI) remaining). For complete reduction of 1 mM U(VI), 0.5 mM of lactate is consumed while 0.5 mM of acetate is generated according to Equation (4). While the change in lactate concentration from 20 mM to 19.5 mM is minor in the given systems, the acetate concentration will increase by 25% from 2.0 to 2.5 mM acetate over the course of U(VI) reduction. However, calculations showed that this change will not affect U(VI) speciation above pH 5.5 for the given experimental conditions.

Equation (4) also shows that reduction of 1 mM UO_2^{2+} will increase the dissolved inorganic carbon concentration in the reactors by 0.5 mM HCO_3^-. Midway through the reduction reaction, an increase of the DIC concentration by 5% or less based on the initial concentration can be considered minor in the systems containing 5.0 to 50 mM DIC (Table 1). For the system starting with 1 mM DIC and 1 mM U(VI), the change of U(VI) speciation from the onset to the midpoint of the reduction reaction was checked with MINEQL. At pH 6.3, the results showed a slight increase in the percentage of the predominant complex $(UO_2)_2CO_3(OH)_3^-$ from 88.3 to 90.9%, and a change of the second-most abundant complex from initially $(UO_2)_3(OH)_5^+$ (6.3%) to $UO_2CO_{3(aq)}$ (4.7%). To conclude, for all experimental systems studied the relative change of U(VI) speciation during U(VI) reduction can be considered negligible.

Speciation calculations indicated that all mineral phases for which thermodynamic data were included in the database were undersaturated. For the calcium-containing systems, calcite was predicted to be undersaturated for all but one condition (5 mM calcium at pH 6.8), where the saturation index was slightly positive. However, during the short time course of the experiment, the formation of calcite at SI $< +0.5$ is considered to be unlikely. This was also confirmed by ICP-OES analysis of the filtered suspension that revealed constant Ca concentrations over the course of the experiment.

Reaction Product Characterization

The uranium product formed by *Shewanella oneidensis* MR-1 through bioreduction has previously been identified by means of synchrotron based X-ray powder diffraction (SR-PD), extended X-ray absorption fine structure (EXAFS) spectroscopy, and high-resolution transmission electron microscopy (HR-TEM) (Bargar et al. 2008; Schofield et al. 2008; Ulrich et al. 2009; Ulrich et al. 2008; Veeramani et al. 2009). The combined results indicated extracellular nanoparticles of 2–5 nm diameter with a mineral structure and composition homologous to stoichiometric UO_{2+x} (with $x < 0.05$) and were consistent with bacteriogenic UO_2 described in other studies, e.g., by Burgos et al. (2008), Marshall et al. (2009) (all using *Shewanella oneidensis* MR-1), and Singer et al. (2009) (using *Shewanella putrefaciens* CN32).

U(VI) Reduction at Varied Carbonate Concentrations

The effect of dissolved inorganic carbon on U(VI) reduction was studied in the DIC concentration range from 1.0 to 50 mM at a fixed pH of 6.3 in Ca-free systems (Table 1). Although uranium was almost entirely reduced in all reactors, the reaction rates varied considerably with the concentration of carbonate amendment. While in the presence of 1 mM DIC U(VI) reduction was complete within 3 h of reaction (Figure 2a), 3.8% of the initial U(VI) remained after 20 h of reaction in the presence of 50 mM DIC (not shown). For most systems, the reduction was complete within 4 to 6 hours, thus the reduction rate constants were calculated based on the data up to 4 h of reaction time (Table 1). Within this time frame, an almost log-linear decrease of [U(VI)] suggests pseudo-first-order kinetics with respect to

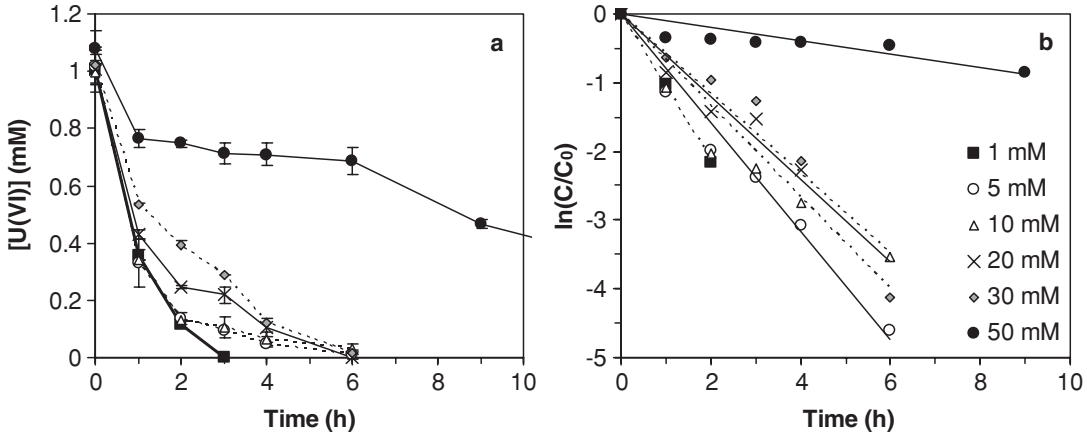

FIG. 2. (a) Concentration of U(VI) versus time for different DIC concentrations. (b) The plot of ln([U(VI)/[U(VI)]$_0$) versus time suggests a pseudo-first-order dependency of U(VI) reduction with respect to [U(VI)]. Reaction conditions: [U(VI)]$_0$ of 1.0–1.1 mM, pH 6.3, no calcium, mean cell density of 21 $\pm$ $2 \cdot 10^7$ cells/mL.

U(VI) (Figure 2b). The U(VI) reduction rates are inversely correlated to the DIC concentration (Figure 3a) and likewise to the total concentration of U(VI)carb complexes (Figure 3b), which are the dominant species in the carbonate-containing systems at 1 mM DIC and higher. Interestingly, the U(VI) reduction rate constants are positively correlated to the logarithm of the total concentrations of U(VI)hyd and U(VI)org complexes (Figure 3c).

U(VI) Reduction at Varied Calcium Concentrations and pH

The effect of dissolved calcium on U(VI) reduction was studied in the concentration range from 0 to 5 mM calcium at two pH conditions, pH 6.3 (using a fixed [DIC] of 35 mM) and pH 6.8 ([DIC] fixed to 42 mM). At both pH conditions, U(VI) reduction significantly slowed down with increasing Ca concentration, clearly demonstrating an inhibitory effect of calcium (Figure 4a, c). At pH 6.3 in the absence of Ca, U(VI) was not detectable in the reactor after 20 h, but for this same pH and reaction time, 22% of the initial U(VI) remained in the system amended with 5 mM calcium and even 0.7% of the initial U(VI) was left after three days. At pH 6.8, the reduction reaction was completely suppressed within the first 6 h of the experiment when using a five-fold stoichiometric excess of calcium compared to dissolved U(VI) (Figure 4c, 4d). For the other experimental conditions, a roughly log-linear decrease of [U(VI)] suggests a pseudo–first-order kinetics with respect to U(VI) (Figure 4b, d).

Comparing the U(VI) reduction rates with respect to pH, lower rate constants were found at pH 6.8 than at pH 6.3 (Figure 4b, d), and the lowest rate was found at pH 8 (Table 1).

The reduction rate constants are inversely related to the calcium concentration (Figure 3d). The pH change from 6.3 to 6.8 caused a negative shift of the linear regression function along the y-axis while maintaining the slope of the curve at about -0.035. A similar result is found when plotting against the total concentration of CaU(VI)carb complexes (Figure 3e). Using the data of all three tested pH conditions, the U(VI) reduction rate constants are again positively correlated to the logarithm of the total concentrations of U(VI)hyd and U(VI)org complexes (Figure 3f).

DISCUSSION

U(VI) Reduction Rates and Energetic Effects

The results clearly demonstrated that U(VI) speciation controls the kinetics of U(VI) reduction by *Shewanella oneidensis* MR-1. Based on the thermodynamic data, the reduction of all U(VI) species considered in our systems is energetically feasible. Differences in the microbial reduction kinetics can be caused by differences in the energetics of the overall reaction, variation in the oxidation-reduction potential, or by species-specific reaction kinetics.

For both sets of experiments, the Ca-free systems with varied DIC concentration (Figure 3c) and the systems with varied calcium and fixed DIC concentration (Figure 3f), our results show a positive correlation of the U(VI) reduction rate constants with the logarithm of the total concentration of U(VI)hyd and U(VI)org complexes, which are in turn related to the logarithm of the UO_2^{2+} concentration. The trend with the logarithm of the concentration may indicate that the speciation affects the rate constant by affecting the Gibbs free energy of the reaction or the redox potential for the reduction of U(VI).

The rate constants show a strong linear correlation with the calculated potential of the UO_2^{2+} reduction half-reaction for both the Ca-free (Figure 5a) and the Ca-containing systems at pH 6.3 (Figure 5c). In both these systems, E_H spans a relatively wide range among the different experimental conditions (67 mV and 54 mV, respectively). Merging both data sets into one plot maintains the positive correlation (Figure 6b). However, at higher pH

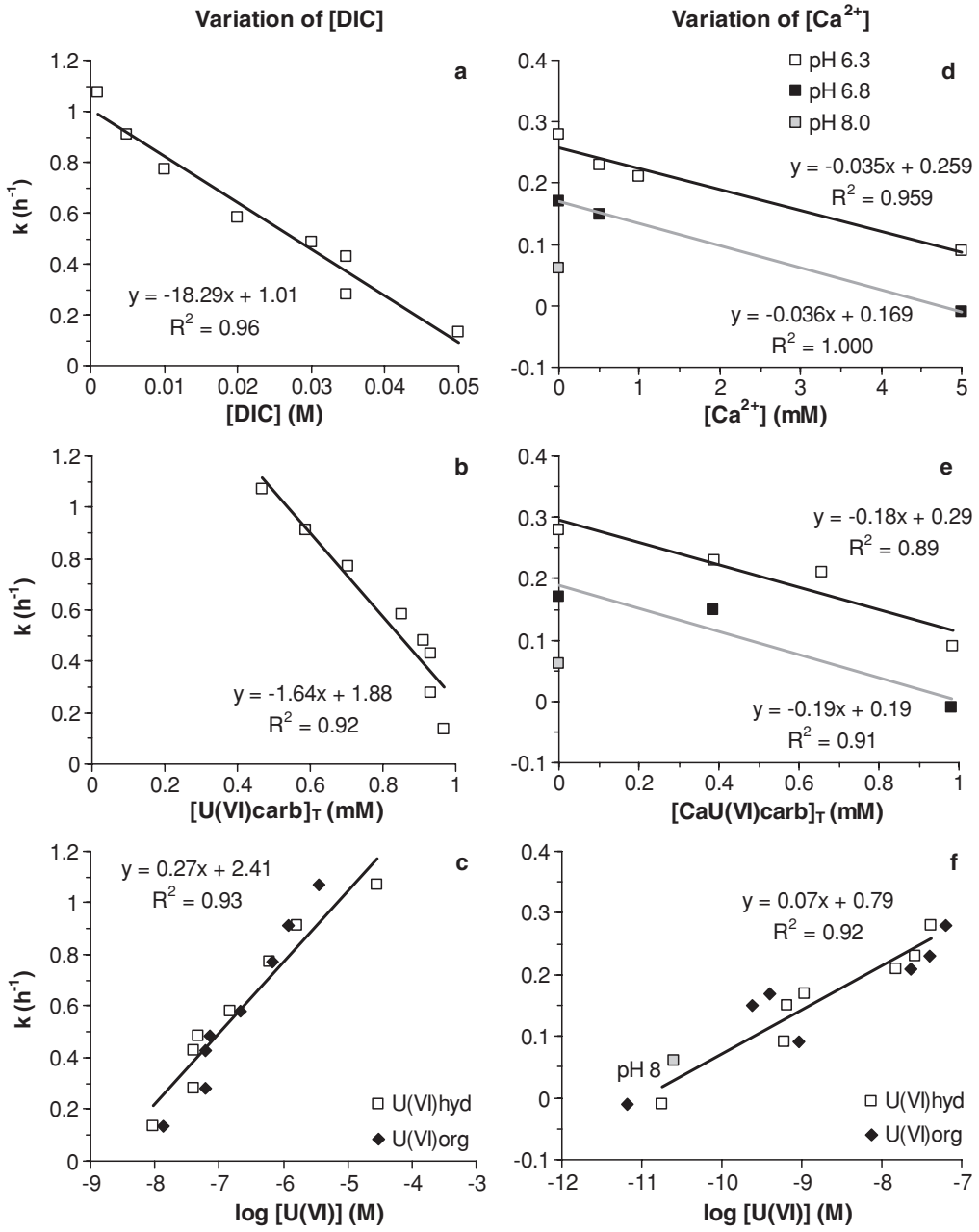

FIG. 3. Correlation between U(VI) reduction rate constants k and the total concentrations of (a) dissolved inorganic carbon, (b) U(VI)carb complexes, (c) logarithm of total concentrations of U(VI)hyd (open squares) and U(VI)org complexes (filled diamonds) for Ca-free systems with varied [DIC] at pH 6.3, and total concentration of (d) Ca^{2+}, (e) CaU(VI)carb complexes, and logarithm of total concentrations of U(VI)hyd and U(VI)org complexes (same symbols as in panel c), for systems with varied pH and calcium concentration at fixed [DIC]. All data collected for $[U(VI)]_0 = 1$ mM. R^2 is the correlation coefficient.

the E_H becomes more negative, resulting in slower U(VI) reduction (Table 1, Figure 5c). Together, these observations suggest that the redox potential can be a major rate-controlling factor.

A possible explanation for these observations is that differences in the E_H are related to the kinetics of one specific step in a possible chain of steps involved in the electron transfer from the cell to U(VI), and this would be the rate-limiting step. Similar correlations of reduction reaction rates with the E_H of the electron acceptor have been observed for the abiotic reduction of organic contaminants (Schwarzenbach et al. 2003).

Equivalent to the E_H, ΔG_r will change linearly with the logarithm of $[UO_2^{2+}]$ if all other factors are held constant (according to Eq. 4). Consistent with this prediction, the U(VI) reduction rate constants show a linearly rising trend with an increasing absolute value of Gibbs free energy of reaction for both the Ca-free (Figure 5b) and the Ca-containing systems (Figure 5d), and

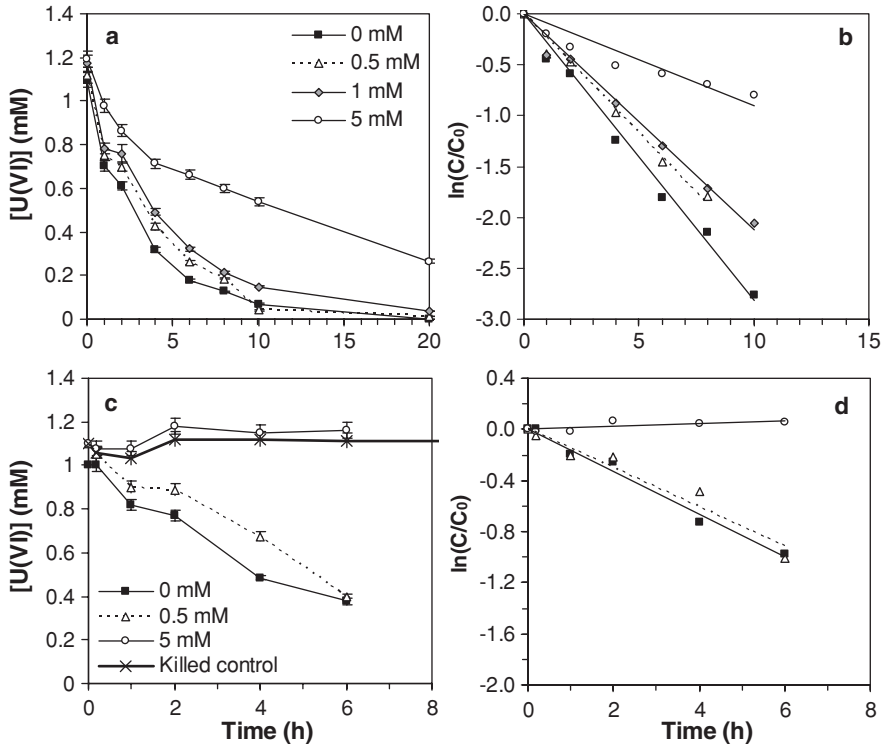

FIG. 4. Concentration of U(VI) versus time for different calcium concentrations at (a) pH 6.3 ± 0.02 and [DIC] of 35 mM, and (c) pH 6.8 ± 0.02 and [DIC] of 42 mM. The linear regressions of ln([U(VI)/[U(VI)]$_0$) versus time (panels b and d) suggest a pseudo–first-order dependency of U(VI) reduction with respect to [U(VI)]. Reaction conditions: [U(VI)]$_0$ of 1.1–1.2 mM, mean cell density of $21 \pm 2 \cdot 10^7$ cells/mL.

when merging both data sets collected at pH 6.3 into one plot (Figure 6c).

However, compared to the overall high level of ΔG_r up to −600 kJ/mol, the differences in ΔG_r among the different conditions were rather small (variation over a range of only 44 kJ/mol) (Table 1). It is unlikely that these minor differences in Gibbs free energy would lead to measurable differences in U(VI) reduction rates. It is not surprising that the rate constants correlate linearly with both the E_H and the ΔG_r, because the Gibbs free energy of an overall reaction is proportional to the difference between the E_H values of the electron donor and electron acceptor half-reactions and because the electron donor half-reaction (lactate oxidation to acetate) is essentially independent of the solution chemistry for the conditions studied.

U(VI) Reduction Rates and Speciation

An important question to consider is whether the most dominant or the most labile (but minor) U(VI) species in a given system will be rate-limiting for microbial U(VI) reduction. For example, in calcium-containing experiments at pH 6.3 and 6.8, the CaU(VI)carb species comprise 99% of [U(VI)]$_0$, but k has a positive correlation with the concentration of the minor U(VI)hyd and U(VI)org complexes (as shown in Figure 3f). Apart from energetic effects such as redox potential and Gibbs free energy of reaction, the rates of U(VI) reduction by *Shewanella oneidensis* MR-1 can be controlled by species-specific reaction kinetics, for example, ligand-dependent accessibility of the U(VI) center atom for electron transfer.

Although our experiments have covered a significant range of different conditions in terms of [DIC], [Ca], and pH, the conditions were not sufficiently numerous or varied to determine individual kinetic constants for all the 24 U(VI) complexes considered (i.e., 11 U(VI)hyd, 7 U(VI)carb, 2 CaU(VI)carb and 4 U(VI)org species). However, our experimental conditions were varied enough to examine three or four critical factors that control U(VI) reduction kinetics. To solve Equation (3), the conditional groups of U(VI)hyd and U(VI)org complexes were combined because their concentrations co-varied too much to allow resolution of separate rate constants. The following k values were obtained for the conditional groups of U(VI)hyd/org, U(VI)carb, and CaU(VI)carb complexes: $k_{(1+2)} = 10.9\ h^{-1}$, $k_3 = 0.459\ h^{-1}$, and $k_4 = 0.015\ h^{-1}$.

Although these rate constants are conditional and each constant corresponds to a group of multiple U(VI) species, order of magnitude differences are apparent among the conditional groups. In particular, these numbers demonstrate that microbial reduction was fastest for the U(VI)hyd/org species, 24 times faster than reduction of the U(VI)carb complexes and 735-times faster than reduction of the CaU(VI)carb complexes. Because the agreement between experimental and calculated k-rates (fitted from Eq. (3)) was fairly good but not exceptional (Figure 7), these results should not be over-interpreted.

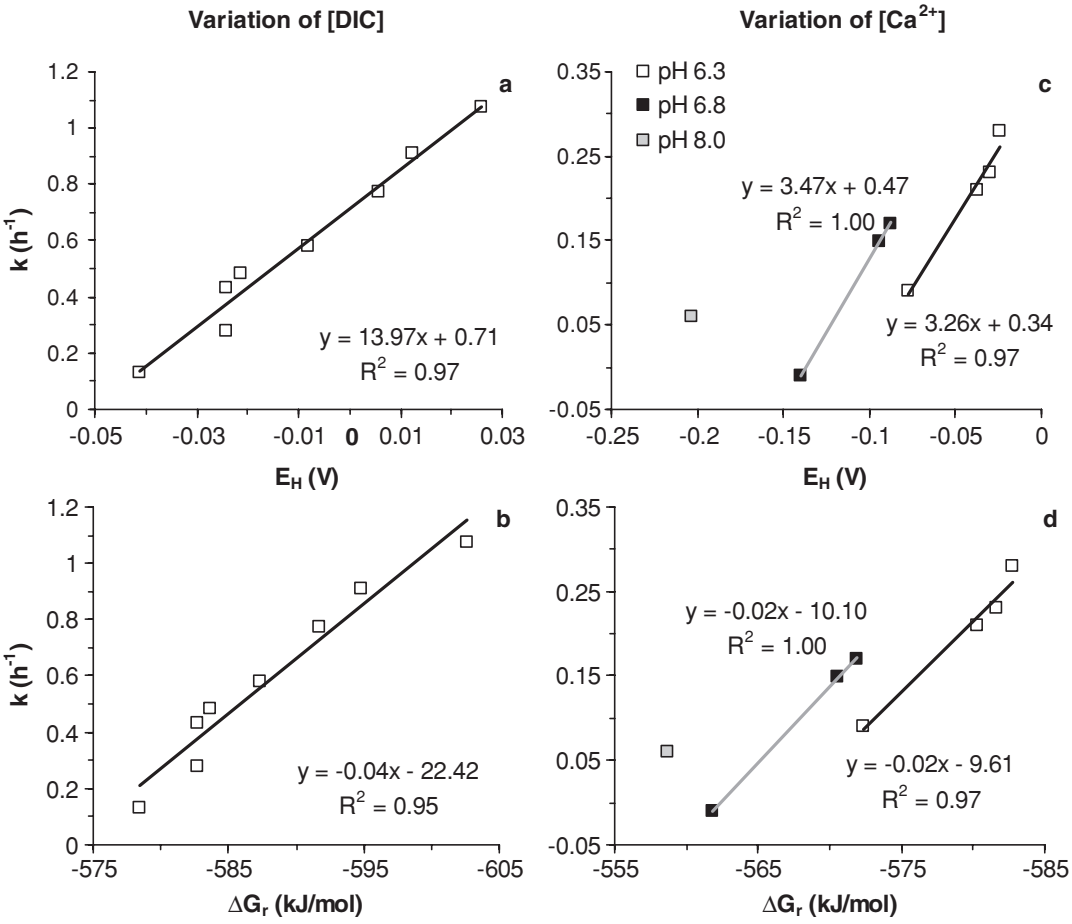

FIG. 5. Correlation between U(VI) reduction rate constants k and redox potential for the reduction of UO_2^{2+} (panel a and c), and Gibbs free energy of reaction (b and d) for Ca-free systems with varied [DIC] at pH 6.3 (a and b), and for systems with varied pH and calcium concentration at fixed [DIC] (c and d; symbols indicate different levels of pH). All data collected for $[U(VI)]_0$ of 1 mM. R^2 is the correlation coefficient.

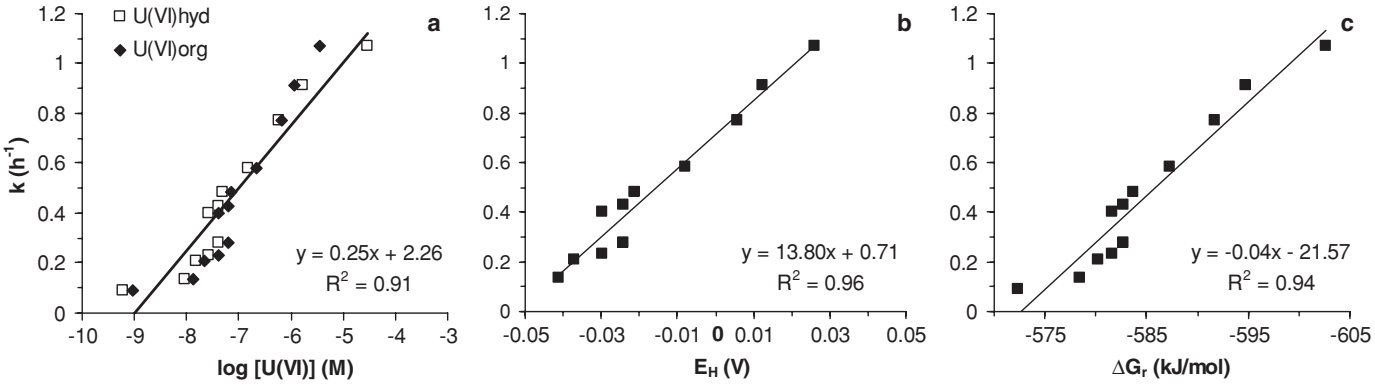

FIG. 6. For the experimental systems at pH 6.3, merging the data of the Ca-containing and Ca-free systems causes only a minor change of the linear regression curves for the correlation between U(VI) reduction rate constants k and (a) the logarithm of total concentration of U(VI)hyd complexes (open squares) and U(VI)org complexes (filled diamonds) (compare to Fig. 3c); (b) the redox potential for the reduction of UO_2^{2+} (compare to Fig. 5a); and (c) the Gibbs free energy of reaction (compare to Fig. 5b). R^2 is the correlation coefficient.

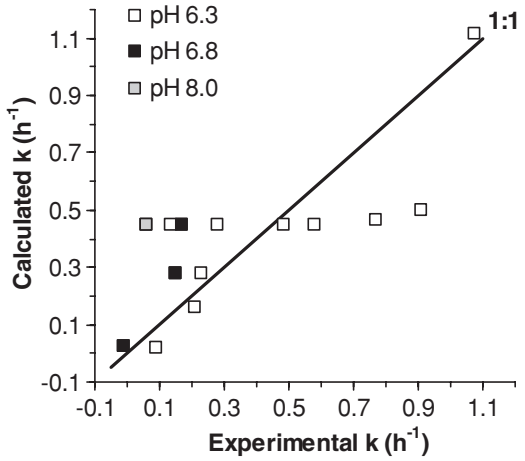

FIG. 7. Correlation between experimental U(VI) reduction rate constants *k* and those calculated from Equation (3) for all conditions (Table 1). Open squares refer to pH 6.3, black squares to pH 6.8, and the grey square to pH 8.0; black line indicates linear slope of 1.0.

One reason for the deviation of calculated from experimental rate constants is that the individual U(VI) species within each conditional group can have different reduction rate constants. Changes in the proportion of these species would thus change the overall reaction rate. This effect is illustrated for the change of U(VI) speciation as a function of DIC concentration at pH 6.3 (Figure 8). With increasing [DIC], the predominance of the aqueous complex $(UO_2)_2CO_3(OH)_3^-$ decreases while $UO_2(CO_3)_2^{2-}$ and, above 17 mM DIC, $UO_2(CO_3)_3^{4-}$ become the dominant U(VI) complexes in this system (Figure 8a). Interestingly, when relating the calculated concentration of $(UO_2)_2CO_3(OH)_3^-$ and $UO_2(CO_3)_3^{4-}$ to the reduction rate, positive and negative trends were found, respectively (Figure 8b and 8c). This observation suggests that while U(VI)carb complexes are bioavailable, the reaction kinetics of individual U(VI)carb complexes can be quite different.

Due to the limited variety of chemical conditions and a more semi-quantitative approach, any reasoning on possible mechanisms causing these differences in the reaction kinetics must

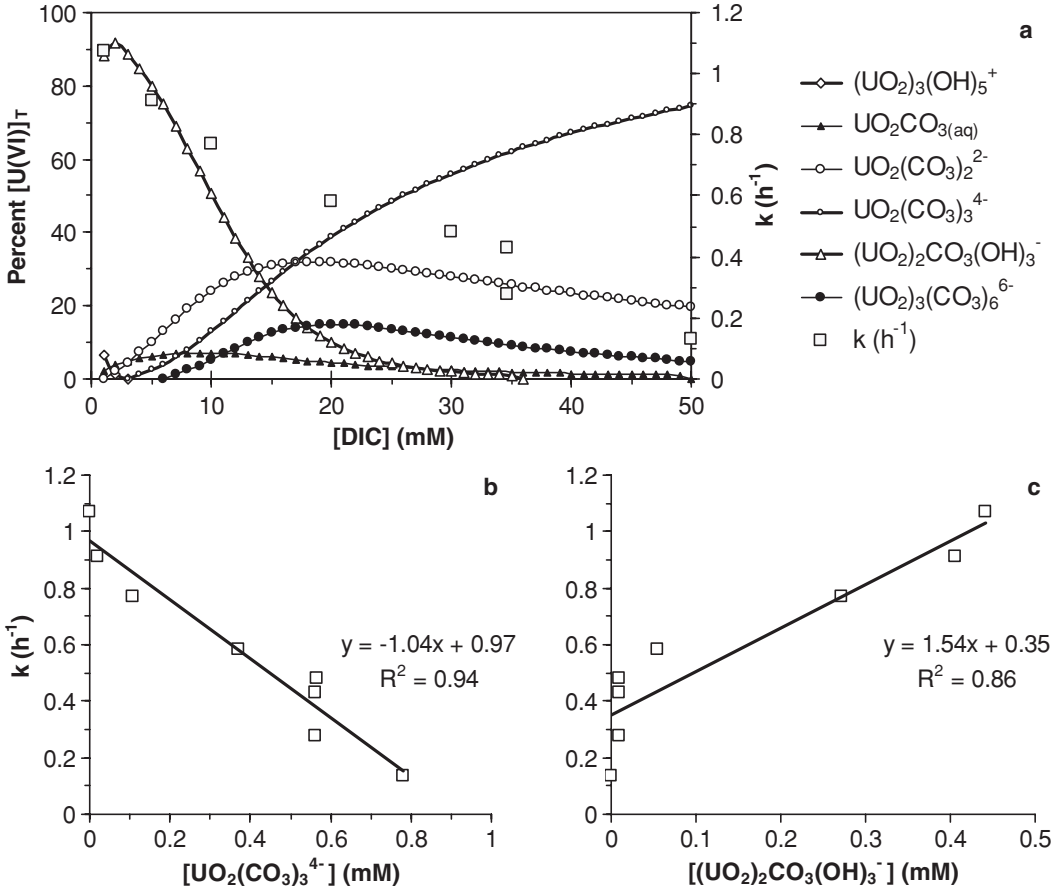

FIG. 8. (a) U(VI) aqueous speciation as a function of DIC concentration for Ca-free closed systems at pH 6.3 containing 1 mM uranyl acetate and 20 mM lactic acid. Only species with ≥3% significance are shown; solids were not considered in speciation calculation. Microbial U(VI) reduction rate constants *k* are drawn as open squares on the right ordinate. The two panels below show the correlation between *k* and the calculated concentration of (b) $UO_2(CO_3)_3^{4-}$ and (c) $(UO_2)_2CO_3(OH)_3^-$ in these systems. R^2 is the correlation coefficient.

remain speculative. One possible explanation is that the U(VI) atom needs to have its coordination environment sufficiently changed (e.g., by removing CO_3^{2-} ligands) to allow electron transfer. A similar explanation was suggested for microbial Fe(III) reduction by Haas and DiChristina (2002), who suggested that reduction of the fully uncoordinated metal ion would be the rate limiting step in Fe(III) reduction.

The correlations between k and E_H for systems with or without calcium indicate that calcium does not have any effect on U(VI) reduction other than the formation of Ca-U(VI)-carbonate complexes. In particular, a direct inhibitory effect of calcium on U(VI) reduction (e.g., by inhibiting the enzymes' catalytic sites or the electron donor) can be ruled out, consistent with the conclusion by Brooks et al. (2003) who showed that contrary to the reduction of U(VI), reduction of fumarate or pertechnetate ($Tc(VII)O_4^-$) was unaffected by the presence of calcium under identical conditions.Stewart et al. (2007) hypothesized that the (enzymatic) U(VI) reduction by *S. putrefaciens* may be sterically hindered or subject to a high activation energy barrier associated with the dissociation of the calcium-uranyl-carbonate complex.

Whereas the hypothesis appears well founded that the redox potential is responsible for the slow reduction of CaU(VI)carb complexes (Brooks et al. 2003), further investigation is needed to unravel whether lower affinity of the U(VI)carb species to the reductase, differences in ligand exchange kinetics, and/or hindered electron transfer to the U(VI) atom in comparison to U(VI)hyd species are responsible for the observed decrease in the rate of microbial U(VI) reduction caused by carbonate.

Comparison with Microbial Fe(III) Reduction Kinetics

A similar biochemical system in which the speciation of a dissolved metal influences its rate of reduction is the reduction of Fe(III) by *Shewanella* species. The rates of reduction of soluble Fe(III) complexes by *Shewanella oneidensis* MR-1 decreased in the order of Fe(III)-EDTA > Fe(III)-NTA > Fe(III)-citrate, which is the same order as the strengths of these complexes (Ross et al. 2009). The faster reduction rates occurred for the most stable Fe(III)-complexes (i.e., Fe(III)-EDTA). The reduction of all three complexes is thermodynamically favorable and the differences in the free energies of reduction for the complexes were not substantial, so other differences among soluble complexes are responsible for the different rates.

Computational chemistry calculations demonstrated that measured rates of soluble Fe(III) reduction by purified cytochromes produced by *Shewanella oneidensis* MR-1 correlated well with the differences in reorganization energies for the Fe(III) complexes associated with electron transfer reactions (the components pertaining to nuclear rearrangement within the precursor complex). Reorganization energies are influenced by the stoichiometry, size, charge, and structure of the Fe(III)-organic complex (Wang et al. 2008). In contrast to the studies with *Shewanella oneidensis* MR-1, reduction rates with *Shewanella putrefaciens* CN32 increased with decreasing strength of 1:1 Fe(III) complexes with citrate, NTA, EDTA, 5-sulfosalicylate, salicylate, and tiron (catechol-3,5-disulphonic acid). Although the 1:1 complex was not the dominant complex over the conditions studied (non 1:1 complexes were dominant), the authors suggested that the rates could inversely correlate with the strength of the 1:1 complex because of its relationship to the rates of ligand exchange and its potential role as the species interacting with the terminal reductase (Haas and Dichristina 2002).

CONCLUSIONS

The kinetics of U(VI) reduction by *Shewanella oneidensis* MR-1 are strongly affected by U(VI) speciation, which will be controlled by the aqueous geochemistry of a given environmental setting. As the speciation of U(VI) changes with variation in pH, [DIC], and $[Ca^{2+}]$, so do the rates of microbial U(VI) reduction. This investigation demonstrated decreasing U(VI) reduction rates with increasing calcium concentrations (as expected) as well as with increasing DIC concentrations. While this trend is consistent with studies published on abiotic systems, it may appear surprising for biotic systems in which carbonate is routinely used for pH buffering and as a complexing agent to prevent precipitation of U(VI) minerals like schoepite during microbial U(VI) reduction. However, according to our study, carbonate is not essential for U(VI) bioreduction by *Shewanella oneidensis* MR-1.

For the range of conditions studied in this work, there are two possibilities that can explain the reduction rate dependency on U(VI) speciation. (a) Rates are governed by the E_H of the UO_2^{2+} reduction half-reaction, which can be the terminal and rate-limiting step in the electron transfer from the bacteria to U(VI). (b) Different U(VI) species have different rate constants. Because the experimental conditions of this study were not different enough to determine individual kinetic constants for all of the 24 U(VI) complexes considered, conditional rate constants were optimized for four groups of U(VI)-ligand complexes. This approach revealed that U(VI) reduction rates were fastest for the groups of U(VI)-hydroxyl and U(VI)-organic complexes (lumped together for fitting purposes), and 24-times slower for the group of U(VI)-carbonate complexes. A semi-quantitative analysis suggests different reactivity of U(VI) species within the U(VI)-carbonate group.

Our investigation also demonstrates that a relatively minor change in pH from 6.3 to 6.8 can significantly slow down the rate of microbial U(VI) reduction. This effect was primarily caused by the decrease in concentration of the most labile U(VI)-hydroxyl species that showed the highest group-specific rate constant.

The results of this study are relevant to microbial as well as chemical U(VI) reduction in subsurface environments for the purposes of *in situ* remediation, as they demonstrate the importance of U(VI) speciation in controlling reduction kinetics. In chemical environments with elevated concentrations of carbonate, and in the presence of calcium, decreased rates of U(VI) reduction are expected. Other important factors controlling U(VI)

speciation and thus rates of microbial U(VI) reduction are E_H and pH. Interestingly, *Shewanella oneidensis* MR-1 reduced uranium in the presence of calcium at a pH close to 7. This finding can potentially be important for bioremediation applications where the presence of calcium inhibits U(VI) reduction by other bacteria.

ACKNOWLEDGMENTS

This research was funded by the U.S. Department of Energy, Office of Basic Energy Sciences grant # DE-FG02-06ER64227, through the linked grants 1027833 (EPFL) and 1027834 (WU). Work carried out at EPFL was funded in part by the Swiss NSF grant # 20021-113784. We wish to thank all collaborators within the joint DOE project, in particular John Bargar (Stanford Synchrotron Radiation Lightsource) and Brad Tebo (Oregon Health & Science University), for valuable discussions.

REFERENCES

Abdelouas A, Lutze W, Nuttall HE. 1999. Uranium contamination in the subsurface: Characterization and remediation. In: Burns PC, Finch R, eds. Uranium: Mineralogy, geochemistry and the environment. Reviews in Mineralogy. Washington, DC: Mineralogical Society of America. P 433–474.

Anderson RT, Vrionis HA, Ortiz-Bernad I, Resch CT, Long PE, Dayvault R, Karp K, Marutzky S, Metzler DR, Peacock A, White DC, Lowe M, Lovley DR. 2003. Stimulating the in situ activity of *Geobacter* species to remove uranium from the groundwater of a uranium-contaminated aquifer. Appl Environ Microb 69:5884–5891.

Bargar JR, Bernier-Latmani R, Giammar DE, Tebo BM. 2008. Biogenic uraninite nanoparticles and their importance for uranium remediation. Elements 4:407–412.

Behrends T, Van Cappellen P. 2005. Competition between enzymatic and abiotic reduction of uranium(VI) under iron reducing conditions. Chem Geol 220:315–327.

Brooks SC, Fredrickson JK, Carroll SL, Kennedy DW, Zachara JM, Plymale AE, Kelly SD, Kemner KM, Fendorf S. 2003. Inhihition of bacterial U(VI) reduction by calcium. Environ Sci Technol 37:1850–1858.

Burgos WD, McDonough JT, Senko JM, Zhang GX, Dohnalkova AC, Kelly SD, Gorby Y, Kemner KM. 2008. Characterization of uraninite nanoparticles produced by *Shewanella oneidensis* MR-1. Geochim Cosmochim Acta 72:4901–4915.

Dong WM, Brooks SC. 2006. Determination of the formation constants of ternary complexes of uranyl and carbonate with alkaline earth metals (Mg^{2+}, Ca^{2+}, Sr^{2+}, and Ba^{2+}) using anion exchange method. Environ Sci Technol 40:4689–4695.

Fredrickson JK, Zachara JM, Kennedy DW, Duff MC, Gorby YA, Li S-MW, Krupka KM. 2000. Reduction of U(VI) in goethite (α-FeOOH) suspensions by a dissimilatory metal-reducing bacterium. Geochim Cosmochim Acta 64:3085–3098.

Gu BH, Wu WM, Ginder-Vogel MA, Yan H, Fields MW, Zhou J, Fendorf S, Criddle CS, Jardine PM. 2005. Bioreduction of uranium in a contaminated soil column. Environ Sci Technol 39:4841–4847.

Guillaumont R, Fanghänel T, Fuger J, Grenthe I, Neck V, Palmer DA, Rand MH. 2003. Update on the chemical thermodynamics of uranium, neptunium, plutonium, americium and technetium. Amsterdam: Elsevier. 919 p.

Haas JR, Dichristina TJ. 2002. Effects of Fe(III) chemical speciation on dissimilatory Fe(III) reduction by *Shewanella putrefaciens*. Environ Sci Technol 36:373–380.

Hua B, Xu HF, Terry J, Deng BL. 2006. Kinetics of uranium(VI) reduction by hydrogen sulfide in anoxic aqueous systems. Environ Sci Technol 40:4666–4671.

Jeon BH, Dempsey BA, Burgos WD, Barnett MO, Roden EE. 2005. Chemical reduction of U(VI) by Fe(II) at the solid-water interface using natural and synthetic Fe(III) oxides. Environ Sci Technol 39:5642–5649.

Liu CX, Gorby YA, Zachara JM, Fredrickson JK, Brown CF. 2002. Reduction kinetics of Fe(III), Co(III), U(VI) Cr(VI) and Tc(VII) in cultures of dissimilatory metal-reducing bacteria. Biotechnol Bioeng 80:637–649.

Liu CX, Jeon BH, Zachara JM, Wang ZM, Dohnalkova A, Fredrickson JK. 2006. Kinetics of microbial reduction of solid phase U(VI). Environ Sci Technol 40:6290–6296.

Lloyd JR, Chesnes J, Glasauer S, Bunker DJ, Livens FR, Lovley DR. 2002. Reduction of actinides and fission products by Fe(III)-reducing bacteria. Geomicrobiol J 19:103–120.

Lovley DR, Phillips EJP, Gorby YA, Landa ER. 1991. Microbial reduction of uranium. Nature 350:413–416.

Luo J, Weber FA, Cirpka OA, Wu WM, Nyman JL, Carley J, Jardine PM, Criddle CS, Kitanidis PK. 2007. Modeling in-situ uranium(VI) bioreduction by sulfate-reducing bacteria. J Contam Hydrol 92:127–146.

Marshall MJ, Dohnalkova AC, Kennedy DW, Plymale AE, Thomas SH, Löffler FE, Sanford RA, Zachara JM, Fredrickson JK, Beliaev AS. 2009. Electron donor-dependent radionuclide reduction and nanoparticle formation by *Anaeromyxobacter dehalogenans* strain 2CP-C. Environ Microbiol 11:534–543.

Moore RC, Borkowski M, Bronikowski MG, Chen JF, Pokrovsky OS, Xia YX, Choppin GR. 1999. Thermodynamic modeling of actinide complexation with acetate and lactate at high ionic strength. J Sol Chem 28:521–531.

Moskvin AI. 1969. Complex formation of the actinides with anions of acids in aqueous solutions. Radiokhimiya 11:458–460.

N'Guessan AL, Vrionis HA, Resch CT, Long PE, Lovley DR. 2008. Sustained removal of uranium from contaminated groundwater following stimulation of dissimilatory metal reduction. Environ Sci Technol 42:2999–3004.

Neiss J, Stewart BD, Nico PS, Fendorf S. 2007. Speciation-dependent microbial reduction of uranium within iron-coated sands. Environ Sci Technol 41:7343–7348.

Ortiz-Bernad I, Anderson RT, Vrionis HA, Lovley DR. 2004. Resistance of solid-phase U(VI) to microbial reduction during in situ bioremediation of uranium-contaminated groundwater. Appl Environ Microb 70:7558–7560.

Partanen JI, Juusola PM, Minkkinen PO. 2003. Determination of stoichiometric dissociation constants of lactic acid in aqueous salt solutions at 291.15 and at 298.15 K. Fluid Phase Equilib 204:245–266.

Ross DE, Brantley SL, Tien M. 2009. Kinetic characterization of OmcA and MtrC, terminal reductases involved in respiratory electron transfer for dissimilatory iron reduction in *Shewanella oneidensis* MR-1. Appl Environ Microb 75:5218–5226.

Sawyer CN, McCarty PL, Parkin GF. 2003. Chemistry for Environmental Engineering and Science, 5th Ed. New York: McGraw-Hill. 752 p.

Schecher WD, McAvoy DC. 1998. MINEQL$^+$: A chemical equilibrium modeling system, version 4.5. Hallowell, ME: Environmental Research Software.

Schofield EJ, Veeramani H, Sharp JO, Suvorova E, Bernier-Latmani R, Mehta A, Stahlman J, Webb SM, Clark DL, Conradson SD, Ilton ES, Bargar JR. 2008. Structure of biogenic uraninite produced by *Shewanella oneidensis* strain MR-1. Environ Sci Technol 42:7898–7904.

Schwarzenbach RP, Gschwend PM, Imboden DM. 2003. Environmental organic chemistry, 2nd Ed. Hoboken, NJ: Wiley. 752 p.

Senko JM, Istok JD, Suflita JM, Krumholz LR. 2002. In-situ evidence for uranium immobilization and remobilization. Environ Sci Technol 36:1491–1496.

Singer DM, Farges F, Brown GE. 2009. Biogenic nanoparticulate UO_2: Synthesis, characterization, and factors affecting surface reactivity. Geochim Cosmochim Acta 73:3593–3611.

Stewart BD, Neiss J, Fendorf S. 2007. Quantifying constraints imposed by calcium and iron on bacterial reduction of uranium(VI). J Environ Qual 36:363–372.

Suzuki Y, Suko T. 2006. Geomicrobiological factors that control uranium mobility in the environment: Update on recent advances in the bioremediation of uranium-contaminated sites. J Mineral Petrol Sci 101:299–307.

Ulrich KU, Ilton ES, Veeramani H, Sharp JO, Bernier-Latmani R, Schofield EJ, Bargar JR, Giammar DE. 2009. Comparative dissolution kinetics of biogenic and chemogenic uraninite under oxidizing conditions in the presence of carbonate. Geochim Cosmochim Acta 73:6065–6083.

Ulrich KU, Singh A, Schofield EJ, Bargar JR, Veeramani H, Sharp JO, Bernier-Latmani R, Giammar DE. 2008. Dissolution of biogenic and synthetic UO_2 under varied reducing conditions. Environ Sci Technol 42:5600–5606.

Veeramani H, Schofield EJ, Sharp JO, Suvorova EI, Ulrich KU, Metha A, Giammar DE, Bargar JR, Bernier-Latmani R. 2009. Effect of Mn(II) on the structure and reactivity of biogenic uraninite. Environ. Sci. Technol 43:6541–6547.

Wang ZM, Liu CX, Wang XL, Marshall MJ, Zachara JM, Rosso KM, Dupuis M, Fredrickson JK, Heald S, Shi L. 2008. Kinetics of reduction of Fe(III) complexes by outer membrane cytochromes MtrC and OmcA of *Shewanella oneidensis* MR-1. Appl Environ Microb 74:6746–6755.

Wu WM, Carley J, Gentry T, Ginder-Vogel MA, Fienen M, Mehlhorn T, Yan H, Caroll S, Pace MN, Nyman J, Luo J, Gentile ME, Fields MW, Hickey RF, Gu BH, Watson D, Cirpka OA, Zhou JZ, Fendorf S, Kitanidis PK, Jardine PM, Criddle CS. 2006. Pilot-scale in situ bioremedation of uranium in a highly contaminated aquifer. 2. Reduction of U(VI) and geochemical control of U(VI) bioavailability. Environ Sci Technol 40:3986–3995.